Chemistry–A European Journal
Research Article
doi.org/10.1002/chem.202301474
Chemistry Europe
European Chemical Societies Publishing
www.chemeurj.org

Special Collection

Covalently Modified MoS_2 Bearing a Hamilton-Type Receptor for Recognizing a Redox-Active Ferrocene-Barbiturate Guest via Multiple H-Bonds

Ioanna K. Sideri,[a] Christina Stangel,[a] Anastasios Stergiou,[a] Alexandra Liapi,[a] Hiram Joazet Ojeda-Galván,[b] Mildred Quintana,[b] and Nikos Tagmatarchis*[a]

Dedicated to Prof. Maurizio Prato on the occasion of his 70th birthday.

Abstract: The covalent modification of the metallic phase of MoS_2 with a Hamilton-type ligand is presented, transforming MoS_2 to a recognition platform which is able to embrace barbiturate moieties via hydrogen bonding. The successful hydrogen bonding formation is easily monitored by simple electrochemical assessments, if a ferrocene-labeled barbiturate analogue is utilized as a proof of concept. Full spectroscopic, thermal, and electron microscopy imaging characterization is provided for the newly formed recognition system, along with valuable insights concerning the electrochemical sensing. The given methodology expands beyond the sensing applications, confidently entering the territory of supramolecular interactions on the surface of 2D transition metal dichalcogenides. The well-designed host-guest chemistry presented herein, constitutes a guide and an inspiration for hosting customized-structured functional building blocks on MoS_2 and its relatives via hydrogen bonding, opening up new opportunities regarding potential applications.

Introduction

Molecular recognition by supramolecular host-guest interactions is in the spotlight of chemistry and nanoscience. It provides a toolkit for multiple applications, ranging from nanocarriers to sensing.[1] Recently, we highlighted the molecular recognition of sodium ions by two-dimensional (2D) molybdenum disulfide (MoS_2) nanosheets, covalently functionalized with a crown ether.[2] Performing selective supramolecular complexation of the analyte on the surface of nanostructured materials holds the potential of minimizing undesired side interactions. Especially, in the case of electrochemically active transition metal dichalcogenides (TMDs), likewise MoS_2, grafting guest-molecules, as recognition motifs for the desired analyte, should enable the fabrication of highly sensitive sensors. As a plus, 2D TMDs are flexible, easy to process and even easier to integrate in complex systems. In general, two-dimensional materials have been widely studied as candidates for bio- and environmental sensing applications.[3] Up to date, MoS_2, the mostly explored TMD, has been investigated as biosensing platform, owing to its structure-dependent unique optical, electrochemical and electronic properties, that are also tailored upon functionalization.[4] In this context, a range of analytes have been successfully detected by MoS_2-based electrochemical probes, including glucose,[5] dopamine,[6] adenine and guanine,[7] hyaluronic acid,[8] thrombin and adenosine triphosphate,[9] chloramphenicol,[10] H_2O_2,[11] and DNA.[12]

Barbiturates belong to a class of organic compounds that are widely used as sedative-hypnotic medications for combating sleep and anxiety disorders, treating epilepsy and non epileptic seizures as well as as anesthetics.[13,14] Barbiturates and their close relatives, cyanurates, are also used in non-pharmaceutical activities, including flame retardants,[15] disinfectants or bleaches for example,[16] and even drug abuse. Therefore, their direct detection via highly sensitive sensors has become an urgent need. Hamilton was the first one to recognize the ability of these heterocyclic systems to form hydrogen bonds and introduced the later-called Hamilton-type receptors;[17] organic molecules that can selectively accommodate natural barbiturate-based molecules and their analogues via hydrogen-bonding.[18] This strategy has been used for supramolecular fabrication of materials[19] and molecular recognition-driven processes (i.e. catalysis, electron transfer).[20] Hamilton receptors

[a] I. K. Sideri, Dr. C. Stangel, Dr. A. Stergiou, A. Liapi, Dr. N. Tagmatarchis
Theoretical and Physical Chemistry Institute
National Hellenic Research Foundation
48 Vassileos Constantinou Avenue, 11635 Athens (Greece)
E-mail: tagmatar@eie.gr
[b] Dr. H. J. Ojeda-Galván, Dr. M. Quintana
High Resolution Microscopy-CICSaB and Faculty of Science
Universidad Autonóma de San Luis Potosi
Av. Sierra Leona 550, 78210 Lomas de San Luis Potosi, SLP (Mexico)

Supporting information for this article is available on the WWW under https://doi.org/10.1002/chem.202301474

This article is part of a joint Special Collection in honor of Maurizio Prato.

are synthesized by cheap readily available starting materials and offer the major advantage of providing different anchoring groups. The ease of chemical design enabled the implementation of Hamilton-type receptors in the preparation of supramolecular dendrimers,[21] self-assembled monolayers on gold,[22–24] polymers with barbiturate selective sites,[25] metal-organic catalysts with barbiturate recognition sites,[26–28] and host-guest complexation-driven photoinduced charge transfer processes, in fullerene-based donor-acceptor dyads[29] and triads.[30] However, their incorporation in 2D nanomaterials has been non-existent, except for a recent important report on Hamilton receptor building blocks on semiconducting monolayer graphene, designed for selective recognition of barbiturates and cyanurates.[31] The successful sensing was realized with the fabrication of a field-effect transistor that could transduce the hydrogen bonding into shift in the electrical signal. In light of the technical development of 2D nanomaterials towards specific applications, graphene is slowly leaving the scene, while transition metal dichalcogenides have gained enormous interest, represented by the head of the family, MoS_2.

In the meantime, the incorporation of the Hamilton-type receptor remains elusive as far as TMDs are concerned, while also the metallic phases of these 2D nanomaterials have been in the spotlight, owing to their conductive properties and functionalization capability.[32] Complying with the research narrative, our approach introduces the molecular host-guest interaction system on the metallic phase of chemically exfoliated MoS_2 for the first time, while a redox-active indicator is ab initio incorporated on the barbiturate moiety as a proof of concept of the successful hydrogen bonding. Herein, we present a novel strategy, including the first covalent functionalization route for decorating modified exfoliated MoS_2 nanosheets with a Hamilton receptor and a redox-active barbiturate derivative. In parallel, the immobilization of the custom-designed barbiturate derivative on the surface of MoS_2 is realized via multiple hydrogen bonds. Accordingly, this work is a guide and an inspiration to hosting customized-structured functional building blocks on MoS_2 and its relatives via hydrogen bonding, opening new avenues on its potential applications.

In order to evaluate the performance of the host-guest complexation on the surface of the Hamilton-modified MoS_2 nanosheets, we synthesized a barbituric acid derivative labelled with ferrocene (Fc), which served as a redox probe for monitoring the molecular recognition event. In fact, Fc has been tested in the past as integral part of a Hamilton-type receptor for the electrochemical detection of barbital.[33] In our investigation, we took advantage of the superior charge transport properties of two-dimensional MoS_2 towards the synthesis of nanosheets decorated by covalently grafted Hamilton-receptors, acting as potential functional electrodes. In this context, the host-guest complexation of the redox-active Fc labelled barbituric acid was monitored by the electrochemical response of the hybrid MoS_2 electrode. This material architecture is based on the selective molecular recognition of the analyte by the electrochemical sensor via multiple supramolecular interactions, in contrast to plasmonic- and transistor-based sensors, which mainly enhance the amplitude of the recorded current without selectivity. In addition, the proposed approach constitutes an appealing strategy to construct MoS_2 based nanomaterials bearing any functionality by taking advantage of the well-designed host-guest chemistry. Customized barbiturate analogues may carry properties and functions of choice and when trapped by the Hamilton receptor, share those with the MoS_2-based system, enabling numerous applications apart from sensing. Herein, the successful recognition of the Fc-labeled barbiturate analogue is a proof of concept for this exact idea.

Results and Discussion

Chemically exfoliated MoS_2 (**ce-MoS_2**) nanosheets were prepared by treating bulk MoS_2 with *n*-BuLi solution in hexane.[2] While electrons are transferred form *n*-BuLi to MoS_2, the negative charges generated on its surface are stabilized by the Li^+ cations.[36] It becomes feasible then, that, MoS_2 acts as nucleophile enabling its chemical modification in the presence of an electrophile. The Hamilton receptor, on the other hand, was prepared according to literature procedures (Figure S1)[21] and was specifically designed to bare the aniline functional group, which can be easily converted to the corresponding electrophilic aryl diazonium salt. Diazonium chemistry has proved to be highly efficient methodology for the decoration of ce-MoS_2 nanosheets with organic ligands of choice.[37,38] Having optimized the diazonium reaction functionalization protocol in our laboratory before,[2] we directly employed here the previously successful protocol. In this case, **ce-MoS_2** serves as platform for anchoring of the Hamilton-type receptor, furnishing the functionalized material **Hamilton-MoS_2**, which can then act as the direct molecular recognition means for barbiturate guests (Scheme 1). In order to probe the host-guest ability of the Hamilton receptor, we rationally designed and synthesized a barbiturate analogue, bearing Fc as redox indicator (Scheme 1).[35] Evidently, Fc's molecular framework stability and its ease of derivatization on the cyclopentadienyl ring are adding to its profound rapid reversible Fc/Fc^+ redox activity, making it an ideal candidate as a building block for the design of tracking/sensing functional systems.[39] In our case, Fc serves as an easy and simple electrochemical tracer to prove the successful trapping of barbiturates by the Hamilton-modified MoS_2 platform via multiple hydrogen bonding. Simply, when the **Hamilton-MoS_2** receptor is dispersed in a solution of Fc-barbiturate guest, hydrogen bonds are formed between the amidic hydrogens of Hamilton receptor and the carbonyl oxygens of the barbiturate moiety, as well as between the hydrogens of barbiturate and the pyridinic nitrogen atoms of the Hamilton receptor (Scheme 1). The six-hydrogen-bonded newly formed system, noted as **Fc/Hamilton-MoS_2**, is a bright example of host-guest chemistry performed on the surface of **ce-MoS_2**.

The efficient functionalization protocol of *n*-BuLi-exfoliated MoS_2 with the aid of diazonium chemistry is well established

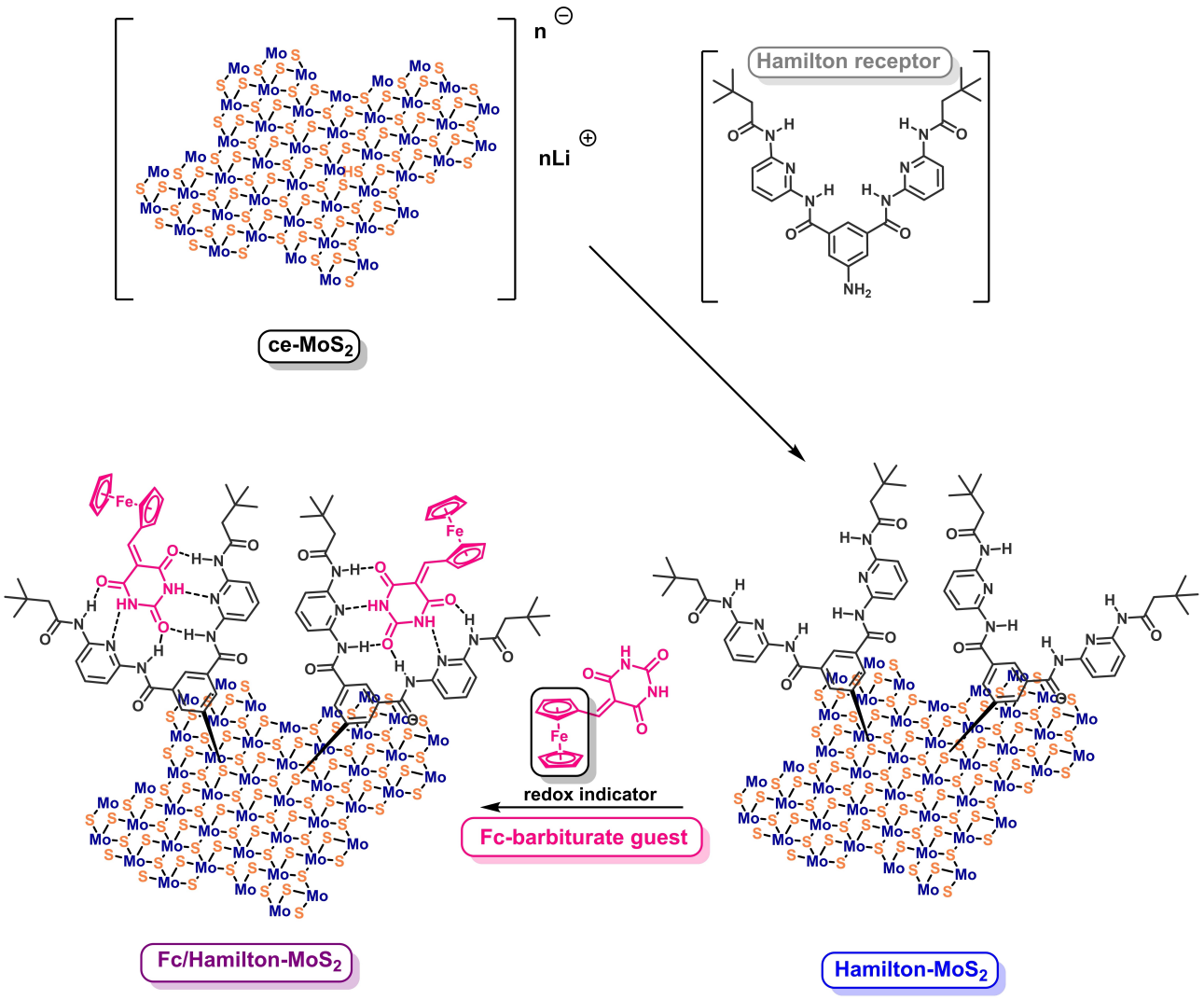

Scheme 1. Modification of **ce-MoS_2**, with a Hamilton-type receptor, towards **Hamilton-MoS_2** material for multiple H-bond recognition of a Fc-barbiturate guest forming **Fc/Hamilton-MoS_2**.

both laboratory-wise and characterization-wise. First strong indications are given by simple FTIR spectroscopy (Figure 1a). In the IR spectrum of **Hamilton-MoS_2**, apart from the characteristic vibrations of MoS_2, strong absorption bands are also present due to the Hamilton-type ligand covalently anchored on its lattice. Specifically, the carbonyl stretching vibration at 1640 cm^{-1} as well as the weak N–H symmetric and asymmetric stretching vibrations at 3400 cm^{-1}, accompanied by the extra band at 3060 cm^{-1} of the amides, corroborate the presence of the Hamilton-type ligand. Also, aliphatic and aromatic C–H stretching vibrations lie around 3000–2800 cm^{-1}, which are associated with the organic matter loaded on **ce-MoS_2**.

Thermogravimetric analysis (TGA) assays, performed under N_2 constant flow, reveal the unusually large loading achieved upon covalent grafting. According to Figure 1b, **Hamilton-MoS_2** undergoes an around 30% weight loss in the temperature range 300–550 °C. This specific temperature window is chosen based on the weight loss of the Hamilton receptor registered under identical temperature range and atmosphere conditions, that is reflected by the first weight derivative response, where 65% of Hamilton receptor's mass is decomposed. Translating the 30% weight loss of **Hamilton-MoS_2** to organic addend mol percentage with respect to MoS_2, leads to the surprising loading of 12.5% mol Hamilton receptor on MoS_2, which is considerably high bearing in mind the covalent grafting that takes place.

Useful insights regarding the covalent grafting are given by Raman spectroscopy. Figure 1c depicts the resonant, with respect to the energy of the A exciton, Raman spectra (633 nm) of starting material bulk MoS_2, **ce-MoS_2**, **Hamilton-MoS_2**, and **Fc/Hamilton-MoS_2** materials. As expected, the spectroscopic fingerprint of 1T-MoS_2, consisting of the J_1, J_2 and J_3 phonon modes, is present in the spectrum of **ce-MoS_2** as compared to the bulk MoS_2 starting material, confirming the phase transition occurred from 2H-to-1T upon *n*-BuLi exfoliation. Specifically, the J_1 mode lies at 153 cm^{-1}, the J_2 at 225 cm^{-1}, and the J_3 at 329 cm^{-1}.[40] These phonon modes are semi-observable in the

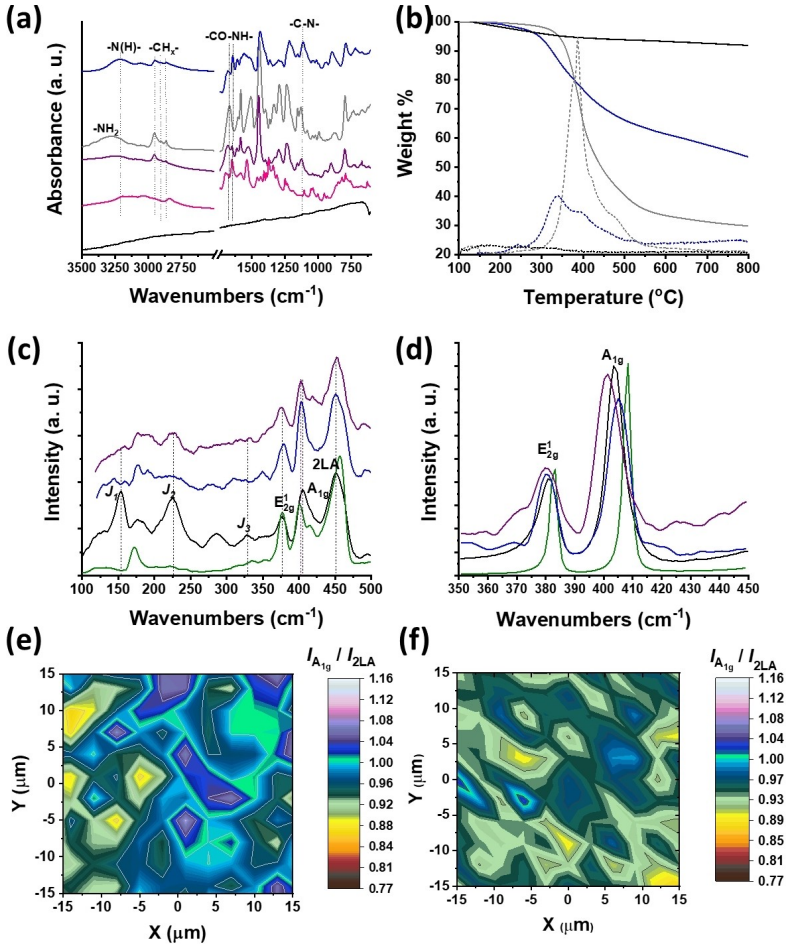

Figure 1. **(a)** FTIR spectra of ce-MoS_2 (black), Hamilton receptor (light grey), Hamilton-MoS_2 (blue), Fc-barbiturate guest (pink), and Fc/Hamilton-MoS_2 (purple). **(b)** TGA graphs and their corresponding 1st weight derivatives (dashed lines) of ce-MoS_2 (black), Hamilton receptor (light grey), Hamilton-MoS_2 (blue), obtained under N_2 constant flow. Raman spectra of ce-MoS_2 (black), bulk MoS_2 (green), Hamilton-MoS_2 (blue), and Fc/Hamilton-MoS_2 (purple), upon excitation at **(c)** 633 nm, and **(d)** 514 nm. Raman intensity ratio $I_{A1g/2LAM}$ spectral maps of a 30 μm × 30 μm area of **(e)** ce-MoS_2 and **(f)** Hamilton-MoS_2.

Raman spectra of the functionalized materials **Hamilton-MoS_2** and **Fc/Hamilton-MoS_2**, with the J_2 being the most intense, while the other two are rather masked. Nevertheless, we deduce that the 1T phase is not entirely lost upon further manipulation. However, the E^1_{2g} mode that is linked to the 2H phase of MoS_2 and is Raman spectroscopically inactive as far as the 1T phase is concerned,[41] is present in all spectra, revealing the coexistence of the two phases in every step. The most important clue though, extracted from Raman spectroscopy, is related to the covalent grafting. Useful information is collected owing to the effect of the local strain induced upon covalent chemical functionalization and the subsequent symmetry disorder. While the 2LAM (second-order longitudinal acoustic phonon in-plane mode) is related to sulfur vacancies, the intensity ratio A_{1g}/2LAM has been broadly utilized as an effective tool to monitor the successful covalent functionalization with sulfur containing organic molecules such as thiols, disulfides, dithiolanes, and dithiolenes, that fill sulfur vacancies, therefore the intensity of the 2LAM band is decreased, while the respective intensity ratio is increased.[42,43] In our case, a different reaction takes place, where a S–C bond is formed (rather than a sulfur vacancy being occupied), when N_2 is released via the diazotization reaction, which affects the structural integrity of the MoS_2 nanosheets, inducing local strain. Similarly with the sulfur vacancy occupation on semiconducting MoS_2, this chemical modification applies also on this type of reaction concerning the metallic phase of MoS_2 and reflects on the intensity ratio A_{1g}/2LAM, based on experimental observations.[2,44] In order to examine this aspect, we performed spatial Raman spectral mapping by acquiring a 30 μm × 30 μm area of MoS_2-based materials and constructing the respective spectral maps of Figure 1e and 1f by plotting the $I_{A1g/2LAM}$ vs the spatial distribution. Indeed, upon functionalization, the $I_{A1g/2LAM}$ mean value is reduced from 0.98 for **ce-MoS_2** (Figure 1c) to 0.92 for **Hamilton-MoS_2** (Figure 1f), which is in agreement with previous reports on diazonium functionalization of MoS_2.[44]

Conversely, the non-resonant, with respect to the energy of the A exciton, Raman spectra (514 nm) provide information related to the phase transition from 2H to 1T upon exfoliation and the layer thickness of the MoS_2 nanosheets produced (Figure 1d). In detail, broadening of the full-width-half-maximum (FWHM) of the A_{1g} mode is observed, namely, a 3.4 cm^{-1}

value is registered for bulk MoS_2 and 4.5 cm^{-1} for **ce-MoS_2**, while **Hamilton-MoS_2** exhibits a value of 8.5 cm^{-1}.[45] In parallel, the frequency difference of A_{1g}–E^1_{2g} was calculated at 25 cm^{-1} for bulk MoS_2, 22 cm^{-1} for **ce-MoS_2** and 21 cm^{-1} for **Hamilton-MoS_2**. These values represent a decrement in the layer thickness of the produced materials, with the exfoliated and functionalized ones being closer to the value of 19 cm^{-1} which is registered for monolayer MoS_2, implying the few-layered nature of the produced samples.[46]

The morphology of **Fc/Hamilton-MoS_2** is evident with the aid of high-resolution transmission electron microscopy (HR-TEM) imaging. In more detail, characteristic TEM micrographs, shown under low magnification in Figure 2a and 2d for **Fc/Hamilton-MoS_2**, reveal the typical structure of the 2D modified MoS_2. Notably, the covalent anchorage of the Hamilton receptor onto MoS_2 leaves undisturbed the 2D nanostructure, evidenced by the absence of defects at the hexagonal MoS_2 lattice (Figure 2c). From the HR-TEM micrograph of Figure 2b–c, it is possible to observe the interlayer MoS_2 separation of 0.65 nm corresponding to the $d_{(002)}$ plane. Moreover, the HR-TEM micrograph of Figure 2c reveals that the atoms exhibit hexagonal atomic arrangement with the d-spacing of 0.27 nm, which is in accordance with the typical $d_{(100)}$ plane of pristine 2H-MoS_2.[47] Fast Fourier transform (FFT) analysis (inset, Figure 2c), was used to elucidate the crystalline nature of MoS_2, within **Fc/Hamilton-MoS_2**. Electron dispersive x-ray spectroscopy (EDS) verifies the presence of Fe, due to the Fc unit recognized by the Hamilton-MoS_2 (Figure 2f), while EDS elemental chemical mapping (Figure 2e) confirms the uniform and aggregation-free distribution of Fc, within **Fc/Hamilton-MoS_2**. The presence of carbon and oxygen at 0.27 and 0.52 keV (Figure 2f), respectively, is due to both the covalently added Hamilton receptor and barbiturate guest and together with the presence of molybdenum and sulfur from MoS_2 (Figure 2f) at 2.3, 17.4 and 2.4 keV, respectively, ensure the successful formation of **Fc/Hamilton-MoS_2**. performed on the surface of **ce-MoS_2**.

Having specifically designed the barbiturate analogue to carry Fc as redox indicator was then feasible to trace electrochemically the hydrogen bonding formation. In order to be able to evaluate properly the expected signals, we first studied the recognition supramolecular system on molecular level, meaning the host Hamilton receptor and the Fc-barbiturate guest separately, as well as their equimolar mix, noted as Fc/Hamilton (1/1) and presented in Figure 3a. This supramolecular complex reference system serves as a guide for the respective results on the nanomaterial level i.e. for 2D MoS_2-based materials. Differential pulse voltammetry (DPV) was the electrochemical method of choice, based on its sensitivity, and all assays were performed in N_2-purged dry benzonitrile. We firstly screened Fc-barbiturate, which shows a reversible oxidation at +0.18 V vs Fc/Fc^+, attributed to the oxidation of Fe^0 to Fe^+ (Figure 3b and Table 1). Hamilton receptor on the other hand, is characterized by one reversible oxidation positioned at +0.88 V vs Fc/Fc^+ (Figure S3a). Conveniently, in the region 0.0–0.5 V vs Fc/Fc^+ no peaks are registered (Figure 3b and Table 1), allowing the clear observation of the potential shift of Fc's half-wave

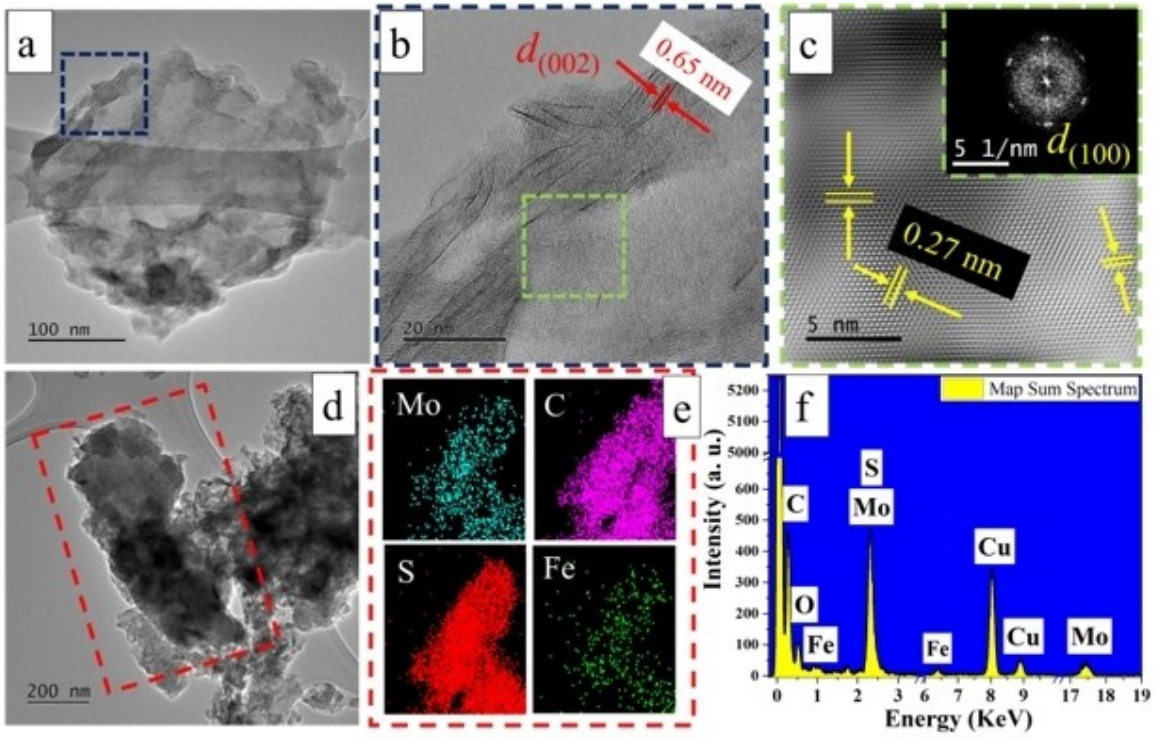

Figure 2. **(a–d)** Representative TEM micrographs of Fc/Hamilton-MoS_2 at low magnification. **(b)** Close up TEM image of Fc/Hamilton-MoS_2 (blue box in Figure 2a) and its interlayer d-spacing. **(c)** HR-TEM micrograph (green box in Figure 2b) and FFT (inset) of Fc/Hamilton-MoS_2. **(e)** EDS elemental chemical mapping (red box in Figure 2d) of Fc/Hamilton-MoS_2. **(f)** EDS spectrum of Fc/Hamilton-MoS_2.

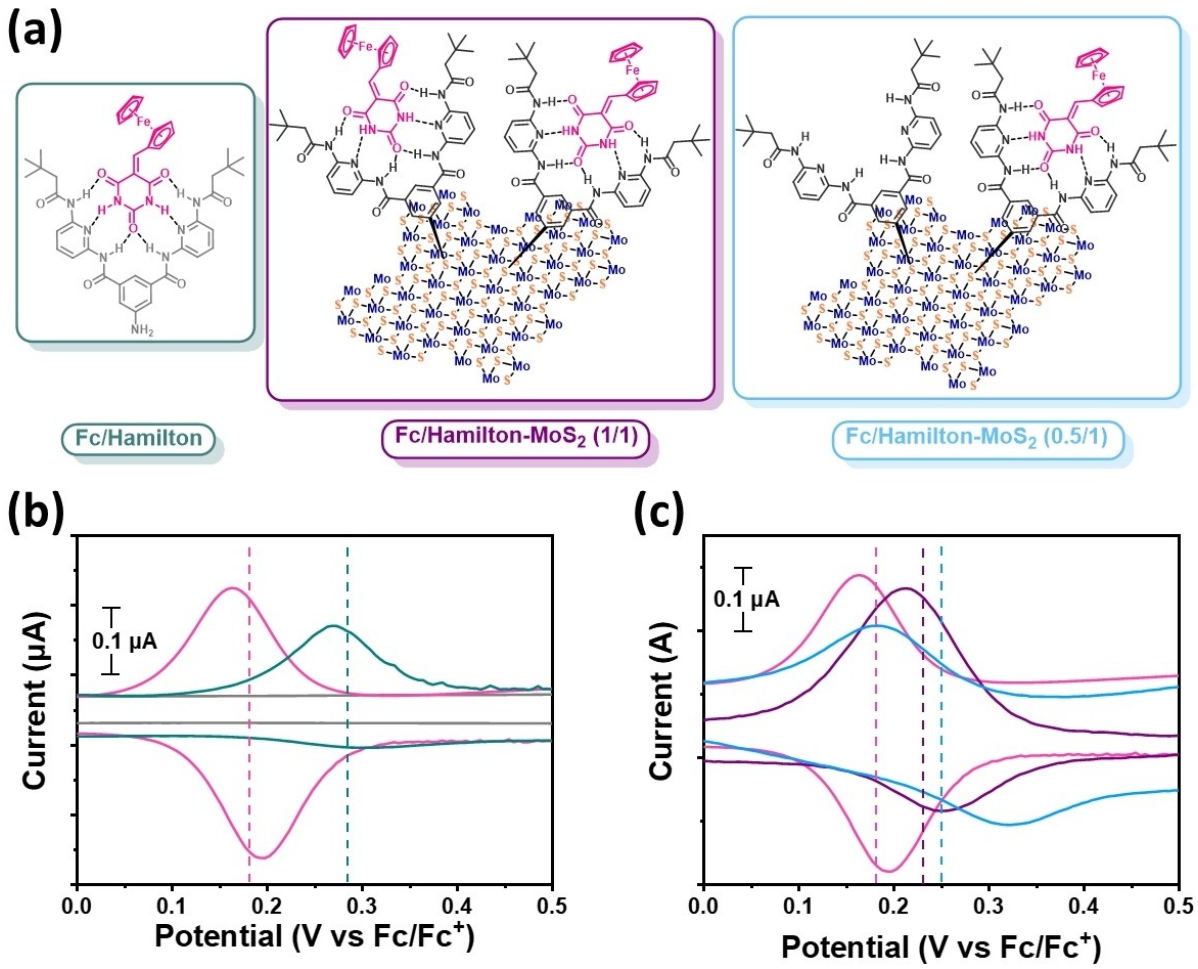

Figure 3. (a) Illustrative scheme of the structures of materials employed in the redox screening. DPV assays of **(b)** Hamilton receptor (light grey), Fc-barbiturate guest (pink), Fc/Hamilton (cyan), and **(c)** Fc-barbiturate guest (pink), Fc/Hamilton-MoS_2 (1 : 1) (purple) and Fc/Hamilton-MoS_2 (0.5 : 1) (light blue). The dashed lines note the half-wave redox potentials. The DPV assays were recorded in N_2-purged dry benzonitrile, with 0.1 M tetrabutylammonium hexafluorophosphate ($TBAPF_6$) in dry benzonitrile as electrolyte and Pt as working, counter and reference electrode.

Table 1. Potential vs Fc/Fc^+ in dry benzonitrile containing 0.1 M $TBAPF_6$ as electrolyte of examined materials. E_{pa}: anodic oxidation potential; E_{pc}: cathodic reduction potential; $\Delta E_{pa,pc}$: potential difference between anodic oxidation potential and cathodic reduction potential; $E_{1/2}$: half-wave potential (average of oxidation and reduction potentials).

Material	$E_{1/2}{}^{Ox}$/V [$\Delta E_{pa,\ pc}$/V]	E_{pa}/V	E_{pc}/V
Fc-barbiturate	+0.18 (0.04)	+0.16	+0.20
Hamilton receptor	+0.88 (0.1)	+0.83	+0.93
Fc/Hamilton	+0.28 (0.02)	+0.29	+0.27
Fc/Hamilton-MoS_2 (1 / 1)	+0.23 (0.04)	+0.21	+0.25
Fc/Hamilton-MoS_2 (0.5 / 1)	+0.25 (0.13)	+0.19	+0.32

redox potential $E_{1/2}$ upon trapping of the Fc-traced barbiturate by the Hamilton receptor. Therefore, upon mixing of the two in 1/1 molar ratio, the Fc/Hamilton (1/1) supramolecular complex is formed via hydrogen bonding, which is characterized by one reversible oxidation at +0.28 V vs Fc/Fc^+ (Figure 3b and Table 1). A shift of 100 mV towards more positive redox potentials is registered for the $E_{1/2}$ of the Fc redox indicator, which implies that upon complex formation, the oxidation of Fc^0 to Fc^+ becomes more difficult, meaning an overpotential is required to reach the next oxidation state. The reasoning behind this effect is twofold. The positive shift is expected, considering the potential electron withdrawing effect of Hamilton receptor amplified by the hydrogen bonding formation. However, the $E_{1/2}$ shift may as well be attributed to the shielding effect due to steric hindrance of the bulk Hamilton receptor that renders the interaction of the electrode with the Fe nucleus, thus holding back the oxidation.[48] In any case, the positive shift registered upon host-guest complexation is also expected on the 2D nanomaterial level. Following this rationale, DPV assays were performed on bare **Hamilton-MoS_2** receptor (Figure S3b), Fc-barbiturate guest and then in varying ratios of the two. With the aid of the TGA, the molar amount of Hamilton receptor on MoS_2 was calculated for a certain mass sample and then equimolar and half equimolar amount of Fc-barbiturate guest were used in order to prepare mixtures of the two in methanol that were sonicated and left stirring for a few minutes. Both samples, **Fc/Hamilton-MoS_2 (1/1)** and **Fc/Hamilton-MoS_2 (0.5/1)** (Figure 3a) were utilized to prepare a MoS_2-based modified electrode on the surface of a conventional Pt

electrode by drop-casting. Note that in both cases not all Fc/barbiturate molecules interact with the Hamilton receptor, meaning that in the case of the 1/1 molar ratio some hosts may be left without guests, while in the case of the 0.5/1 molar ratio, we can only approximately assume that half of the hosts are occupied. Stereochemical factors deriving from the morphological nature of the MoS_2 material may prevent some hosts from successfully accommodating the guests. It should be noted though, that this phenomenon equally affects both estimated ratios, therefore the comparative study between the two is accurate. Nonetheless, in Figure 3a schemes have been drawn this way for presentation purposes. In Figure 3c, the voltamograms of Fc-barbiturate, **Fc/Hamilton-MoS_2 (1/1)**, and **Fc/Hamilton-MoS_2 (0.5/1)** are presented. Complying with the aforementioned narrative, upon host-guest interaction, a positive shift is registered for the reversible oxidation of Fc indicator. Specifically, for **Fc/Hamilton-MoS_2 (1/1)** an extra 50 mV compared to free Fc-barbiturate has to be applied in order for the oxidation to occur owing to the hydrogen bonding (Figure 3c and Table 1). While the shielding and electron withdrawing effects are responsible for this phenomenon, the Fc oxidation actually occurs more easily when the Hamilton receptor is covalently grafted on MoS_2, within **Fc/Hamilton-MoS_2**, vs on the molecular level, system within Fc/Hamilton. The metallic phase of MoS_2 may be the reason behind this observation, since it is characterized by increased electron density and serves as a conductive interlayer promoting electron flow between the electrode and the redox active moiety. On the other hand, **Fc/Hamilton-MoS_2 (0.5/1)** shows a reversible oxidation at $+0.25$ V vs Fc/Fc^+, which is negatively shifted by 30 mV compared to Fc/Hamilton and positively shifted by 20 mV compared to the equimolar mixture **Fc/Hamilton-MoS_2 (1/1)**. The half-equimolar ratio is important to showcase the sensitivity of the method in even less amount of barbiturate. Indeed, a strong shift is registered, even stronger than the one of **Fc/Hamilton-MoS_2 (1/1)**, validating the high sensing activity of the system in decreasing amounts of analyte. The even more difficult oxidation of Fc in excess amount of MoS_2-based receptor is probably linked to the increased steric hindrance that shields the Fe nucleus, resulting in a more positive $E_{1/2}$. However, this very welcome result is accompanied also by reduced current produced, making the recognition slightly less distinct.

Conclusions

In conclusion, host-guest chemical interactions were realized on the surface of chemically exfoliated MoS_2 by covalently grafting a Hamilton-type ligand on its lattice, able to host barbiturate analogues via multiple hydrogen bonding. The successful formation of the six hydrogen-bonded supramolecular complex on MoS_2 was transduced to electrochemical signal owing to a rationally-designed barbiturate labelled with Fc. Upon supramolecular complexation, DPV electrochemical assessments revealed a positive shift on the half-wave redox potential of Fc, validating the initial hypothesis. It is noteworthy, that the sensing capability is possible in even half equimolar amount of barbiturate analyte, with respect to the immobilized Hamilton receptor, with the electrochemical signal produced being rewarding. The predominantly metallic phase of MoS_2 is an ideal conductive surface for electrochemical sensing and while this study describes a prototype methodology for multiple H-bond recognition on the surface of MoS_2, the construction of MoS_2-based electrochemical sensors is proposed. At the same time, this protocol outlines the modification of MoS_2 with ligands of choice, by using non-covalent albeit strong interactions within the recognition motif described. We showcased that barbiturate analogues, appropriately designed to carry ligands of choice, can indeed be trapped within the Hamilton host immobilized on MoS_2. Bearing in mind that hydrogen bonding formation is temperature or solvent-dependent reversible, we believe that switching on and off the host-guest interaction at will, enables MoS_2 to shine in an expanded application field.

Experimental Section

Preparation of the covalently functionalized Hamilton-MoS_2 material: In a round bottom flask, **Hamilton receptor** (280 mg, 0.5 mmol) was dissolved in 5 mL of distilled H_2O followed by the addition of concentrated HCl (100 μL, 1.2 mmol). Then, the resultant solution was cooled in an ice bath and $NaNO_2$ (55 mg, 0.8 mmol) and 0.5 mL HCl 20% were added. The final solution was allowed to stir in the cold bath for 30 min until the color turned to deep yellow indicating the diazonium salt formation. In a round bottom flask, aqueous dispersion of **ce-MoS_2** (~20 mg, 23 mL) was added under nitrogen atmosphere, cooled in an ice bath and allowed to stir. To this dispersion, the cold solution of the in situ generated diazonium salt was added drop-wise and stirred for 2 h in the ice bath, followed by stirring overnight at r.t. Then, the reaction mixture was filtered through a PTFE membrane filter (0.2-μm pore size) and the solid residue was washed thoroughly with copious amounts of distilled water, methanol and acetone (consecutive sonication/filtration cycles) to remove any organic addends. The collected black solid was dried under a high vacuum yielding the functionalized **Hamilton-MoS_2** product.

Preparation of thin-film electrodes Pt/Hamilton-MoS_2, Pt/Fc/Hamilton-MoS_2 (1/1), and Pt/Fc/Hamilton-MoS_2 (0.5/1): The **Hamilton-MoS_2** ink was prepared by dispersing 1.0 mg of the **Hamilton-MoS_2** powder in 600 μL MeOH and sonicated for 30 min prior use. Afterwards, 10 μL aliquot of the **Hamilton-MoS_2** ink were drop casted on the electrode surface and were left to dry at room temperature under vacuum. For **Fc/Hamilton-MoS_2 (1/1)** ink, 3 mg of **Hamilton-MoS_2** and 0.6 mg of **Fc-barbiturate** were dissolved in 2.25 mL MeOH and sonicated for 30 min prior use. Afterwards, 10 μL aliquot of the **Fc/Hamilton-MoS_2 (1/1)** ink were drop casted on the electrode surface and were left to dry at room temperature under vacuum. Similarly, for **Pt/Fc/Hamilton-MoS_2 (0.5/1)** electrode, 3 mg of **Hamilton-MoS_2** and 0.3 mg of **Fc-barbiturate** were dissolved in 2 mL MeOH and sonicated for 30 min prior use. Afterwards, 10 μL aliquot of the **Fc/Hamilton-MoS_2** (0.5/1) ink were drop casted on the electrode surface and were left to dry at room temperature under vacuum.

Acknowledgements

This research is co-financed by Greece and the European Union (European Social Fund – ESF) through the Operational Programme "Human Resources Development, Education and Lifelong Learning 2014–2020" in the context of the project "Chemically modified MoS_2 with organic recognition motifs as electrochemical sensors for the selective detection of ions and (bio)molecules" (MIS 5048201). Thanks are to CONACYT through project A1-S-8817 and the postdoctoral fellowship to H. J. O. G. 2022–2023.

Conflict of Interests

The authors declare no conflict of interest.

Data Availability Statement

The data that support the findings of this study are available from the corresponding author upon reasonable request.

Keywords: barbiturates · Hamilton receptor MoS_2 · host-guest interaction · sensor

[1] G. Yu, K. Jie, F. Huang, *Chem. Rev.* **2015**, *115*, 7240.
[2] A. Stergiou, C. Stangel, R. Canton-Vitoria, R. Kitaura, N. Tagmatarchis, *Nanoscale* **2021**, *13*, 8948.
[3] D. Tyagi, H. Wang, W. Huang, L. Hu, Y. Tang, Z. Guo, Z. Ouyang, H. Zhang, *Nanoscale* **2020**, *12*, 3535.
[4] S. Barua, H. S. Dutta, S. Gogoi, R. Devi, R. Khan, *ACS Appl. Nano Mater.* **2018**, *1*, 2.
[5] N. Rohaizad, C. C. Mayorga-Martinez, Z. Sofer, M. Pumera, *ACS Appl. Mater. Interfaces* **2017**, *9*, 40697.
[6] S. Wu, Z. Zeng, Q. He, Z. Wang, S. J. Wang, Y. Du, Z. Yin, X. Sun, W. Chen, H. Zhang, *Small* **2012**, *8*, 2264.
[7] T. Yang, M. Chen, F. Nan, L. Chen, X. Luo, K. Jiao, *J. Mater. Chem. B* **2015**, *3*, 4884.
[8] W. Gu, Y. Yan, C. Zhang, C. Ding, Y. Xian, *ACS Appl. Mater. Interfaces* **2016**, *8*, 11272.
[9] S. Su, H. Sun, W. Cao, J. Chao, H. Peng, X. Zuo, L. Yuwen, C. Fan, L. Wang, *ACS Appl. Mater. Interfaces* **2016**, *8*, 6826.
[10] R. Yang, J. Zhao, M. Chen, T. Yang, S. Luo, K. Jiao, *Talanta* **2015**, *131*, 619.
[11] H. Kim, H. Kim, C. Ahn, A. Kulkarni, M. Jeon, G. Y. Yeom, M. Lee, T. Kim, *RSC Adv.* **2015**, *5*, 10134.
[12] L. Yan, H. Shi, X. Sui, Z. Deng, L. Gao, *RSC Adv.* **2017**, *7*, 23573.
[13] W. Löscher, M. A. Rogawski, *Epilepsia* **2012**, *53*, 12.
[14] D. J. Cordato, G. K. Herkes, L. E. Mather, M. K. Morgan, *J. Clin. Neurosci.* **2003**, *10*, 283.
[15] N. N. Golovnev, M. S. Molokeey, M. K. Lesnikov, I. V. Sterkhova, V. V. Atuchin, *J. Mol. Struct.* **2017**, *1149*, 367.
[16] F. A. Kappi, G. Z. Tsogas, D. L. Giokas, D. C. Christodouleas, A. G. Vlessidis, *Microchim. Acta* **2014**, *181*, 623.
[17] S. Kyu, Chang, A. D. Hamilton, *J. Am. Chem. Soc.* **1988**, *110*, 1318.
[18] G. Cooke, V. M. Rotello, *Chem. Soc. Rev.* **2002**, *31*, 275.
[19] K. T. Mahmudov, M. N. Kopylovich, A. M. Maharramov, M. M. Kurbanov, A. V. Gurbanov, A. J. L. Pombeiro, *Chem. Rev.* **2014**, *265*, 1.
[20] A. Tron, M. Rocher, P. J. Thornton, J. H. R. Tucker, N. D. McClenaghan, *Asian J. Org. Chem.* **2015**, *4*, 192.
[21] A. Dirksen, U. Hahn, F. Schwanke, M. Nieger, J. N. H. Reek, F. Vögtle, L. De Cola, *Chem. Eur. J.* **2004**, *10*, 2036.
[22] K. Motesharei, D. C. Myles, *J. Am. Chem. Soc.* **1998**, *120*, 7328.
[23] R. Zirbs, F. Kienberger, P. Hinterdorfer, W. H. Binder, *Langmuir* **2005**, *21*, 8414.
[24] C.-K. Liang, G. V. Dubacheva, T. Buffeteau, D. Cavagnat, P. Hapiot, B. Fabre, J. H. R. Tucker, D. M. Bassani, *Chem. Eur. J.* **2013**, *38*, 12748.
[25] E. Loizidou, C. Zeinalipour-Yazdi, L. Sun, *Biomacromolecules* **2004**, *5*, 1647.
[26] J. Larsen, B. S. Rasmussen, R. G. Hazella, T. Skrydstrup, *Chem. Commun.* **2004** 202.
[27] J.-W. Park, J.-H. Park, C.-H. Jun, *J. Org. Chem.* **2008**, *73*, 5598.
[28] Y. Li, Y.-M. He, Z.-W. Li, F. Zhang, Q.-H. Fan, *Org. Biomol. Chem.* **2009**, *7*, 1890.
[29] J. Zhuang, W. Zhou, X. Li, Y. Li, N. Wang, X. He, H. Liu, Y. Li, L. Jiang, C. Huang, S. Cui, S. Wang, D. Zhu, *Tetrahedron* **2005**, *36*, 8686.
[30] N. D. McClenaghan, Z. Grote, K. Darriet, M. Zimine, R. M. Williams, L. De Cola, D. M. Bassani, *Org. Lett.* **2005**, *7*, 807.
[31] L. Bao, B. Zhao, M. Ali, M. Assebban, B. Yang, M. Kohring, D. Ryndyk, T. Heine, H. B. Weber, M. Halik, F. Hauke, A. Hirsch, *Adv. Mater. Interfaces* **2022**, *9*, 2200425.
[32] B. Kirubasankar, Y. S. Won, L. A. Adofo, S. H. Choi, S. M. Kim, K. K. Kim, *Chem. Sci.* **2022**, *13*, 7707.
[33] J. Westwood, S. J. Coles, S. R. Collinson, G. Gasser, S. J. Green, M. B. Hursthouse, M. E. Light, J. H. R. Tucker, *Organometallics* **2004**, *23*, 946.
[34] D. T. Seidenkranz, J. M. McGrath, L. N. Zakharov, M. D. Pluth, *Chem. Commun.* **2017**, *53*, 561.
[35] S. K. Pal, A. Krishnan, P. K. Das, A. G. Samuelson, *J. Organomet. Chem.* **2001**, *827*, 637.
[36] K. C. Knirsch, N. C. Berner, H. C. Nerl, C. S. Cucinotta, Z. Gholamvand, N. McEvoy, Z. Wang, I. Abramovic, P. Vecera, M. Halik, S. Sanvito, G. S. Duesberg, V. Nicolosi, F. Hauke, A. Hirsch, J. N. Coleman, C. Backes, *ACS Nano* **2015**, *9*, 6018.
[37] X. S. Chu, A. Yousaf, D. O. Li, A. A. Tang, A. Debnath, D. Ma, A. A. Green, E. J. G. Santos, Q. H. Wang, *Chem. Mater.* **2018**, *30*, 2112.
[38] C. Gautier, I. López, T. Breton, *Mater Adv* **2021**, *2*, 2773.
[39] G. Roy, R. Gupta, S. R. Sahoo, S. Saha, D. Asthana, P. C. Mondal, *Coord. Chem. Rev.* **2022**, *473*, 214816.
[40] S. Jimenez Sandoval, D. Yang, R. F. Frindt, J. C. Irwin, *Phys. Rev. B* **1991**, *44*, 3955.
[41] D. Yang, S. J. Sandoval, W. M. R. Divigalpitiya, J. C. Irwin, R. F. Frindt, *Phys. Rev. B* **1991**, *43*, 12053.
[42] X. Chen, P. Denninger, T. Stimpel-Lindner, E. Spiecker, G. S. Duesberg, C. Backes, K. C. Knirsch, A. Hirsch, *Chem. Eur. J.* **2020**, *26*, 6535.
[43] I. K. Sideri, R. Arenal, N. Tagmatarchis, *ACS Materials Lett.* **2020**, *2*, 832.
[44] L. Daukiya, J. Teyssandier, S. Eyley, S. El Kazzi, M. Candelaria Rodríguez González, B. Pradhan, W. Thielemans, J. Hofkens, S. De Feyter, *Nanoscale* **2021**, *13*, 2972.
[45] Q. Qian, Z. Zhang, K. J. Chen, *Langmuir* **2018**, *34*, 2882.
[46] C. Lee, H. Yan, L. E. Brus, T. F. Heinz, J. Hone, S. Ryu, *ACS Nano* **2010**, *4*, 2695.
[47] J. Zhou, J. Qin, X. Zhang, C. Shi, E. Liu, J. Li, N. Zhao, C. He, *ACS Nano* **2015**, *9*, 3837.
[48] S. M. Batterjee, M. I. Marzouk, M. E. Aazab, M. A. El-Hashash, *Appl. Organomet. Chem.* **2003**, *17*, 291.

Manuscript received: May 9, 2023
Accepted manuscript online: May 30, 2023
Version of record online: July 12, 2023